This paper proposes an experimental method for studying the Sommerfeld effect in auto-balancers or exciters of resonant vibrations of pendulum, ball, or roller type. The method is based on the processing of signals acquired from analog sensors of rotations and vibration acceleration using regression analysis. The method is tested on a specially designed rotor bench on isotropic viscoelastic supports, which executes spatial motion, and an auto-balancer with one ball.

Checking the accuracy of the method using stroboscopic lighting demonstrates the accuracy of determining the speed of rotation of the rotor, ball, oscillation frequency of the rotor, etc. with an error of several hundredths of a percent.

When fixing the ball relative to the rotor, a classic inertial vibration exciter is obtained. The rotor has two resonant velocities. The Sommerfeld effect is almost not manifested. With a gradual increase in the frequency of the current, the rotor speed increases monotonously. There is no significant slip or jump in the rotor speed. There are two distinct peaks on the amplitude-frequency characteristic. Therefore, such a vibration exciter is not suitable for the excitation of resonant vibrations.

With the free placement of the ball in the oil, the behavior of the system changes significantly in the vicinity of the first resonant velocity. The first narrow resonant peak disappears in the roto. Instead, there is a long, gentle resonant rise. It lasts at a current frequency of 9.4 Hz to 19.3 Hz. The amplitude at the reference point on the resonant rise increases from 0.7 mm to 2.84 mm. Therefore, by changing the frequency of the current, it is possible to smoothly change the amplitude of the rotor oscillations by almost 4 times. The maximum amplitude of rotor oscillations is the same as at the first resonance with a fixed ball. Due to the gentleness of the resonant rise, a freely installed ball itself is a reliable exciter of resonant vibrations

Keywords: inertial vibration exciter, resonant vibratory machine, steady state motion, Sommerfeld effect, autobalancing, motion stability

UDC 531.391.5: 621.928.23
DOI: 10.15587/1729-4061.2022.265578

DETERMINING EXPERIMENTALLY THE PATTERNS OF THE MANIFESTATION OF THE SOMMERFELD EFFECT IN A BALL AUTO-BALANCER

Gennadiy Filimonikhin
Corresponding author
Doctor of Technical Sciences, Professor,
Head of Department*
E-mail: filimonikhin@ukr.net
Volodymyr Yatsun
PhD, Associate Professor
Department of Road Cars and Building**
Anatolii Matsui
Doctor of Technical Sciences, Associate Professor
Department of Automation of Production Processes**
Lubov Olijnichenko
PhD, Senior Lecturer*
Viktor Pukalov
PhD, Associate Professor*
*Department of Machine Parts and Applied Mechanics**
**Central Ukrainian National Technical University
Universytetskyi ave., 8, Kropyvnytskyi, Ukraine, 25006

Received date 01.07.2022
Accepted date 07.09.2022
Published date 21.09.2022

How to Cite: *Filimonikhin, G., Yatsun, V., Matsui, A., Olijnichenko, L., Pukalov, V. (2022). Determining experimentally the patterns of the manifestation of the sommerfeld effect in a ball auto-balancer. Eastern-European Journal of Enterprise Technologies, 5 (7 (119)), 96–104. doi: https://doi.org/10.15587/1729-4061.2022.265578*

1. Introduction

The Sommerfeld effect in the form of a jam at the resonant frequencies of rotor's unbalanced mass or corrective loads is known in vibration and balancing equipment. In balancing equipment, jam modes are undesirable because they interfere with the onset of an autobalancing mode of the motion. In vibration equipment, the Sommerfeld effect is undesirable when accelerating the unbalanced rotors of above-the resonant vibratory machines and is desirable when operating resonant vibratory machines whose work is based on the Sommerfeld effect.

Manifestations of the Sommerfeld effect in various rotary machines are the object of constant studies. The corresponding rotary machines simultaneously have several possible well-established motion modes. Studying their stability is a complex mathematical problem. In addition, the stability of a certain steady state motion can be local. Therefore, the question remains open what motions and how are implemented in practice. Given this, there is a task to experimentally study the Sommerfeld effect in rotary machines.

In the case when the unbalanced mass is rigidly bound to the rotor, there are no fundamental difficulties in investigating this phenomenon. Significant difficulties arise when loads are stuck in the auto-balancer or at the exciter of resonant vibrations of the pendulum, roller, or ball type. In this case, the rotor and load have different speeds of rotation, the loads are inside the body of the auto-balancer or vibration exciter and are not available for visual observation.

Information about the onset of a certain mode of jamming is necessary in practice for designing vibratory machines or auto-balancers, as well as checking their performance.

2. Literature review and problem statement

In 1902, the effect of excitation by an electric motor with an unbalanced rotor of resonant vibrations of an elastic foundation was discovered [1]. The rotor of the motor itself was stuck at a resonant frequency and could not accelerate. The phenomenon was termed the Sommerfeld effect. Fundamentals of the theory of this phenomenon can be found in [2, 3].

They are based on the theory of nonlinear oscillations of mechanical systems [2], in particular, with a limited source of energy [3].

When operating resonant vibratory machines, the Sommerfeld effect is undesirable [4]. It interferes with the acceleration of unbalanced rotors to operating speeds. Therefore, the area of the relevant research is the algorithms for rotor acceleration [5], techniques for passing resonant frequencies [6], etc.

Ways to employ the Sommerfeld effect to design resonant vibratory machines were investigated in the following works:

– [7] – for a dual-mass system, on one of the platforms of which a low-power DC electric motor with a pendulum rigidly mounted on the shaft is installed;

– [8] – for a three-mass system, a wind wheel with an unbalanced mass is installed on one of the platforms.

It was found that the pendulum [7], the wind wheel with an unbalanced mass [8] get stuck at one of the resonant oscillation frequencies of the platform, which excites intense vibrations.

In autobalancing rotary systems, the Sommerfeld effect prevents the onset of autobalancing and is therefore undesirable [9–14]. Manifestations of the Sommerfeld effect in autobalancing systems were investigated in:

– [9] – for the rotor performing spatial motion and a ball auto-balancer;

– [10] – within a flat model of the rotor and a ball auto-balancer;

– [11] – for a rotor with a ball auto-balancer mounted on isotropic supports attached to a massive viscoelastically fixed foundation;

– [12] – for a rotor with a ball auto-balancer rigidly mounted on a viscoelastically fixed platform that performs rectilinear translational motion;

– [13] – for a rotor performing spatial motion and two pendulum auto-balancers;

– [14] – for an electric motor mounted on a viscoelastically fixed platform and a pendulum freely mounted on the shaft of the electric motor.

It was found that loads in the form of balls [9–12] or pendulums [13, 14] can get stuck at one of the resonant oscillation frequencies of the rotor, which executes both flat [10–13] and spatial [9, 13, 14] motions. In this case, the loads are assembled together, which creates a conditional folded load. Thus, in [9], it was found that in the case of one ball auto-balancer, the balls get stuck at the first resonant speed of rotor rotation. In [13], it was found that in the case of two pendulum auto-balancers, the pendulums get stuck at the first and second resonant speeds. From this, we can conclude that one auto-balancer can excite resonant vibrations with the first resonant rotor speed, and two auto-balancers – resonant vibrations with both the first and second resonant frequencies.

However, the possibility of controlling vibrations by changing the rotor speed was not studied in works [9–14].

Taking into consideration the results reported in [9, 10, 13], it is proposed in [15] to use ball, roller, or pendulum auto-balancers as exciters of resonant vibrations. It is clear that when operating a vibratory machine under a resonant mode, the auto-balancing mode is undesirable.

In [16], within the framework of a flat model of a balanced rotor on isotropic supports with an auto-balancer of the ball, roller, or pendulum type, theoretically possible modes of load jamming were determined. In [17], within the framework of a flat model of a balanced rotor on isotropic supports, the excitation of resonant oscillations by a ball, roller, pendulum was investigated. Theoretical research methods and computational experiments establish the local asymptotic stability of various steady state modes of motion of the rotary system.

Such motions can be different modes of jamming, modes of synchronous rotation of loads together with the rotor. Theoretical studies and computational experiments do not make it possible to investigate the area of attraction of each locally asymptotically stable steady state motion. Therefore, the question of which motion will be established over time remains open. The answer to this question, applicable for the design of both auto-balancers and vibration exciters, can only be given by a full-scale experiment.

An experimental study of the Sommerfeld effect in the case of a rotor with an unbalanced mass does not cause fundamental difficulties [18]. Thus, the frequency of the current emitted by the variable-frequency drive is known. The rotor speed is measured by a tachometer. Amplitude of oscillations can be calculated by a signal from an accelerometer. In [18], it was proposed to use wavelet transformations to process digitized signals.

In the case of ball, roller, pendulum auto-balancers or exciters of resonant vibrations, the loads are inside the housing and, therefore, inaccessible for observation. Even if loads (pendulums) are available for observation on a special bench, there are difficulties in accurately determining their jam speeds. Thus, in [13], direct observation of pendulums made it possible to determine that the speed of jamming of pendulums coincides with one of the resonant frequencies of the system. However, this accuracy is not enough to design resonant vibratory machines with a controlled amplitude of oscillations. Therefore, it is advisable to devise methods for studying the Sommerfeld effect in the appropriate rotary machines and test them on a specific bench.

A promising method of processing signals from sensors is the method of regression analysis. It was used in [19] to study the two-frequency vibrations of a single-mass vibratory machine excited by a ball auto-balancer. It is expedient to apply this method to investigate the Sommerfeld effect in the case of auto-balancers or resonant exciters of vibrations of the ball, roller, or pendulum type.

3. The aim and objectives of the study

The aim of this work is to experimentally determine the patterns of manifestation of the Sommerfeld effect in a ball auto-balancer (the exciter of resonant vibrations of the ball type) with a fixed and free installation of the ball in the auto-balancer. This will make it possible to avoid ball jam modes in the auto-balancer as undesirable and provide modes of jamming in resonant vibration exciters of the ball type.

To accomplish the aim, the following tasks have been set:

– to devise methods to experimentally study the Sommerfeld effect for auto-balancers or exciters of resonance vibrations of the ball, roller, or pendulum type; to evaluate the accuracy of methods;

– by using the devised methods, to investigate the Sommerfeld effect with a ball rigidly fixed in the auto-balancer;

– by using the devised methods, to investigate the Sommerfeld effect with a ball freely installed in the auto-balancer.

4. The study materials and methods

4. 1. Bench description

Fig. 1 depicts a diagram of the bench to study the phenomenon of ball jamming. Fig. 2 shows photographs of the bench.

The bench consists (Fig. 1) of a protective casing 1, resting on supports 2. A three-phase induction motor is attached to the casing using the suspension of the induction motor 4 and the rubber viscoelastic sleeve 5.

Induction motor with a power of 180 watts, a rated rotational speed is 1450 rpm. Axisymmetric (isotropic) supports. The shaft of induction motor 6 hosts drum 7 and the body of auto-balancer 8. Inside the auto-balancer is ball 9. In the casing, there is slot 10. Similar gap 11 is in the drum. Lantern 12 through slot 10 provides light inside the casing. Through gap 11, the light gets inside once per twist of the drum. This creates a stroboscopic effect. When the ball lags behind the rotor by 2 times, the image of the ball doubles, and the two balls appear stationary relative to the drum. When the ball lags behind the drum by three, four, etc. times, the image of the ball is tripled, quadrupled, etc. The speed of motor rotation is regulated by variable-frequency drive 13.

The auto-balancer can be used both without a plexiglass lid (Fig. 2, *a*) and with a lid (Fig. 2, *b*). The auto-balancer in the assembly contains a ball filled with oil, closed with plexiglass, which is attached to the body with a ring, disc, and 20 bolts. Synthetic engine oil SAE 5 W-30 (Motul, France) is used.

The mass characteristics of parts or a group of parts of the bench are given in Table 1.

The structure of the auto-balancer housing allows it to be used without a plexiglass lid with oil filling up to 40 ml.

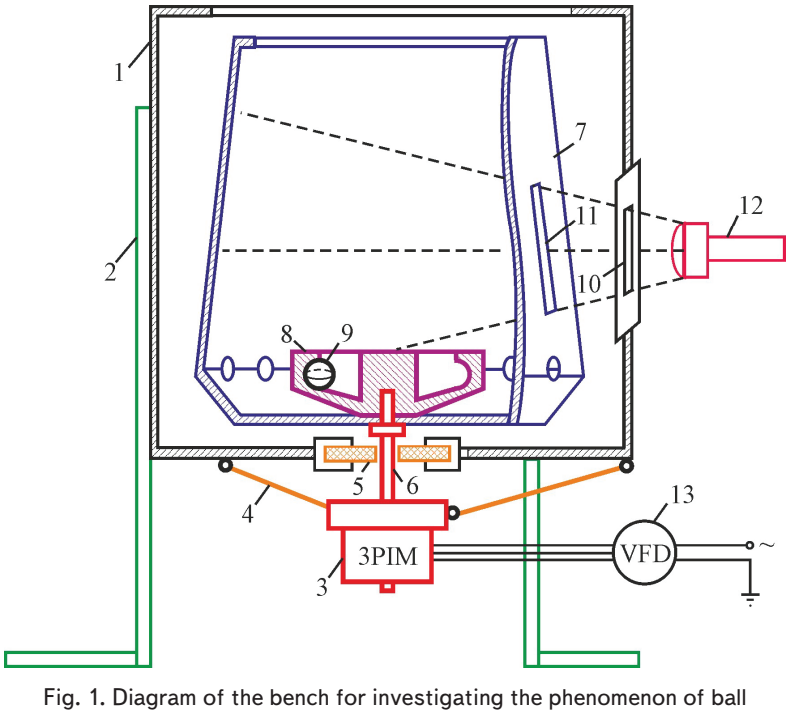

Fig. 1. Diagram of the bench for investigating the phenomenon of ball jamming: 1 — protective cover; 2 — supports; 3 — three-phase induction motor; 4 — lower supports (suspension of the induction motor); 5 — rubber viscoelastic sleeve; 6 — induction motor shaft; 7 — drum; 8 — auto-balancer body; 9 — ball; 10 — gap in the casing; 11 — gap in the drum; 12 — lantern; 13 — variable-frequency drive

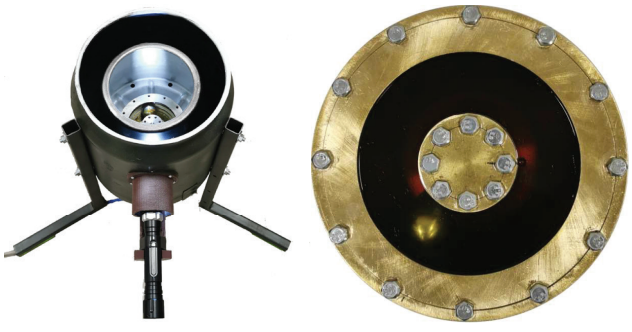

a *b*

Fig. 2. Photograph of the bench for investigating the phenomenon of ball jamming: *a* — bench assembled with an auto-balancer without oil; *b* — auto-balancer assembled, filled with oil

Table 1

Parameters of parts or a group of parts of the bench

No.	Part (group of parts)	Mass, *g*
1	3-phase induction motor, stator	3,149
2	3-phase induction motor, rotor	1,532
3	Auto-balancer housing	1,696
4	Drum	2,145
5	Ring, plexiglass, disc, 20 bolts	318
6	Ball	112
7	Motor oil SAE 5W-30	236

4. 2. Description of equipment, measurement procedure, file of measurement results

Rotating parts in the assembly (drum, induction motor rotor, auto-balancer housing) are balanced dynamically in two correction planes. For this purpose, a portable balancing kit "Balcom-4M" (LLC "Kinematics") is used. It is essential that the rotor is balanced by the reversible components of vibration speed. The ball is in the auto-balancer. 2 ml of oil is added to the body for smooth rolling along the track. The rotor speed is the greatest; the ball lags behind the rotor as much as possible. As a result of dynamic balancing, harmonics corresponding to the current rotor speed disappear.

The vibration state of the bench is characterized by two digitized signals. The first signal is generated by an analog tachometer. The second signal is generated by the analog sensor-accelerometer ADXL335 (Analog Devices, Inc., USA).

An analog tachometer produces an almost constant voltage of 4.8 V for most of one revolution, provided that the laser light does not fall on the white tape. When light hits the white tape, it is reflected and falls on the photoresistor. Because of this, the voltage drops to about 3. 7 V. For each revolution, there is one single pronounced minimum.

The analog accelerometer creates a voltage that varies from 0 to 3.3 V. The sensor is calibrated by acceleration of gravity using standard methods (https://www.analog.com/media/en/technical-documentation/data-sheets/

ADXL335.pdf). For the sensor, the following coefficient of stress transfer to m/s ^{2} was experimentally found:

$$q = 2 \cdot 9.8065 / 0.612 = 32.048 \left[\mathrm{m} / \left(\mathrm{s}^2 \mathrm{V} \right) \right]. \quad (1)$$

Analog signals are digitized by the USB oscilloscope MT Pro 4.1 (MLab, Ukraine). Number of analog channels, 8; ADC bit size, 12 bits; maximum sampling frequency per channel, 500 kHz, when using 7 or 8 channels. The oscilloscope makes it possible to store digitized signals in an Excel file.

The variable-frequency drive makes it possible to change the frequency of the current from 0 to 50 Hz in increments of 0.1 Hz. To obtain a certain steady state motion, a fixed frequency XX.X∈[5.0, 50.0] Hz current is supplied to the induction motor. Once the motion is set, the USB oscilloscope digitizes the corresponding signals. The results are stored in the Excel file "XX.X.xlsm".

The parameters of each steady state motion are recorded with a 2 s oscilloscope with a frequency of 5000 measurements per second. In this case, the Excel file has 3 columns and 10002 rows (Table 2).

Table 2

The structure of the Excel measurement result file

Column/row	*A* (time, s)	*B* (strobe signal, V)	*C* (accelerometer, V)
1	Time	Analog channel 1	Analog channel 2
2	0	4.797827984	1.597877849
3	0.0002	4.7181836245	1.601419018
...	...	...	...
10,002	2	4.782035263	1.375273362

The first line contains the name of the data. The following lines are digital data. In the first column, the time changes in increments Δt=0.0002 s from 0 to 2 s. In the second column, a strobe signal is recorded in V, acquired from the tachometer sensor. In the third column, a signal is recorded in *V*, acquired from the accelerometer sensor.

4. 3. Description of experiments and procedures of their implementation

In experiments, a ball weighing 112 g is used. The ball is placed in the cavity of the auto-balancer. The cavity is completely filled with oil. From above, the cavity is covered with plexiglass. Plexiglas is pressed to the body of the auto-balancer with a ring and disk using 20 bolts. Steady state motions are studied in cases where the ball in the auto-balancer is:

– fixed;

– freely installed.

Various steady state motions of the system corresponding to the current frequency of ν∈[5.0, 50.0] Hz are investigated. All established modes are investigated per one launch of the bench. The frequency of the current varies with alternating increments. A small step of 0.1 Hz is used in the vicinity of resonant velocities. At a distance from resonances, a step of 1, 2, or 5 Hz is used. The resulting Excel files (about 100) are processed using a single procedure.

As a result of processing Excel-files, the following parameters are obtained that characterize the steady state motion:

– $n(\nu)$, Hz or rev/s – rotor speed;

– $n_B(\nu)$, Hz or rev/s – ball rotation speed;

– $A_d(\nu)$, mm – amplitude of oscillations at the control point;

– $\varphi(\nu)$, degree – oscillation phase during synchronous rotation of the ball with the auto-balancer.

According to the parameters found, plots are built characterizing the steady state modes of motion. By comparing the plots in the two experiments, the patterns and features of the manifestation of the Sommerfeld effect in the ball auto-balancer (the ball exciter of resonant vibrations) are established.

5. Results of determining experimentally the patterns of manifestation of the Sommerfeld effect in the ball auto-balancer

5. 1. Methods of experimental study of the Sommerfeld effect for auto-balancers or exciters of resonant vibrations

5. 1. 1. Research methods

The proposed methods for studying the Sommerfeld effect are based on the processing of digitized signals (Table 2) using regression analysis methods.

Signal processing algorithms are implemented in the computer algebra system Mathcad 15. At the same time, it is of no fundamental importance in which algorithmic language or in which programming environment to do it. Mathcad was chosen because of the convenience of controlling calculations, data visualization, etc.

Algorithm 1 – construction of data vectors. By reading data from the Excel file, the vectors of time *t*, strobe signal *s*, acceleration *a* are built:

$$t := \mathrm{READEXEL}(\text{"filename.xlsx"},\text{"A2:A10002"}),$$

$$s := \mathrm{READEXEL}(\text{"filename.xlsx"},\text{"B2:B10002"}),$$

$$a := \mathrm{READEXEL}(\text{"filename.xlsx"},\text{"C2:C10002"}). \quad (2)$$

In (2) "filename.xlsx" is the Excel file title.

Algorithm 2 – determining the number of full revolutions and the average rotor speed at steady state motion. When processing a strobe signal, lines are found from which a new rotation begins. In these lines, the strobe signal is minimal. As a result, a vector *s*0 is built with the corresponding line numbers. The number of revolutions (*Nr*), the average rotational speed per revolution number *i* (n_i, Hz), and at *Nr* revolutions (*n*, Hz) on the steady state motion are determined from the operators:

$$Nr := rows(s0) - 1;$$

$$i := 0,1,\ldots,Nr;$$

$$n_i := 1 / \left[\Delta t \cdot \left(s0_{i+1} - s0_i \right) \right];$$

$$n := Nr / \left[\Delta t \cdot \left(s0_{Nr} - s0_0 \right) \right]. \quad (3)$$

In (3), it is taken into consideration that in Mathcad the elements of the array are numbered with 0.

Algorithm 3 – Determining the number of resonant frequencies and their approximate value. The signals given in Table 2 are recorded within 10 seconds during the run-out of the rotor. According to the Excel file, data vectors are built using example (2).

Algorithm 2 determines the number of full rotor revolutions and average speeds at each revolution. In one figure, using the left and right axes, two plots $a(t)$ and $n(t)$ are constructed. According to the plots, the number of resonant frequencies and their approximate values are determined.

Algorithm 4 – determining the amplitude, phase, and frequency of oscillations during synchronous rotation of the ball with the body of the auto-balancer. Data vectors are built from the Excel file (2). Using the vector s0 (algorithm 2), data are allocated in the Excel file corresponding to *Nr* full rotations. The regression model for acceleration measured in *B*:

$$a(t)=C+A_x\sin(2\pi n_B t)+A_y\cos(2\pi n_B t), \quad (4)$$

where C, A_x, A_y, n_B are the parameters of the nonlinear model to be determined. At the same time, the ball jamming frequency n_B and the coefficients A_x, A_y are of significant importance. They should hardly change when the experiment is repeated.

According to the coefficients A_x, A_y, the amplitude (A_d, mm) and the phase (φ, degrees) of oscillations generated by the ball are determined:

$$A_d=\frac{1{,}000q}{(2\pi n_B)^2}\sqrt{A_x^2+A_y^2},$$

$$\varphi=\begin{cases}(180°/\pi)\cdot\arccos\left(\left|A_x/\sqrt{A_x^2+A_y^2}\right|\right);\\ 180°-\varphi \text{ if } (-A_x<0)\wedge(-A_y>0);\\ 180°+\varphi \text{ if } (-A_x<0)\wedge(-A_y<0);\\ 360°-\varphi \text{ if } (-A_x>0)\wedge(-A_y<0).\end{cases} \quad (5)$$

In (5), q is the coefficient of electrical voltage transfer to m/s^2 from (1). The angle φ is counted from the zero mark (white tape on the drum) towards the rotor rotation.

Algorithm 5 – determining the component of oscillations generated by the ball when lagging behind the rotor. According to the Excel file, data vectors are built (2). A regression model (4) is used for the acceleration measured in *V*. According to the first formula in (5), the amplitude (A_d, mm) of oscillations generated by the ball is determined. Note that when repeating the experiment, the oscillation frequency and amplitude of oscillations should hardly change. The phase of oscillations and coefficients A_x, A_y can change constantly.

Algorithm 6 – determining the slip of the rotor of the induction motor or ball. The sliping of the rotor or ball is determined, respectively, from the formulas

$$s=0.5\nu-n,\quad s_B=0.5\nu-n_B, \quad (6)$$

where ν is the current frequency, n is the rotor speed, n_B is the ball's rotational speed.

Other experiments concern the assessment of the accuracy of research methods. They are partial in nature and are described in the relevant subparagraph.

5. 1. 2. Evaluation of the accuracy of methods

In the experiments, a ball weighing 112 g is used. The ball is freely placed in the body of the auto-balancer. 2 ml of oil are added. The oil provides a soft (without impact) rolling of the ball along the track.

Fig. 3 shows photographs of the auto-balancer in stroboscopic lighting with an exposure of 0. 3 s when lagging behind the rotor by an integer number of times.

When the ball lags behind the rotor by an integer number of times k in stroboscopic lighting, exactly k fixed balls are visible. The rotor speed (rpm) is measured with a tachometer. Dividing it by $60{\cdot}k$ gives the ball jamming speed (rev/s).

a *b* *c* *d*

Fig. 3. Photographs of the auto-balancer in stroboscopic lighting with an exposure of 0.3 s when the ball lags behind the rotor by: *a* – 2 times; *b* – 3 times; *c* – 4 times; *d* – 5 times

Table 3 gives the results of determining the frequency of ball jams, by the described technique and by regression analysis.

Table 3

Comparison of ball jam frequency determined using a tachometer and stroboscopic lighting with the frequency found by regression analysis

Lagging, time	Current frequency ν, Hz	Rotation speed				
		Rotor		Ball, rev/s		
		N, rpm	*n*=*N*/60 rev/s	Stroboscope	Regression analysis	Discrepancy, %
2	16.1	459.5	7.658333	3.829167	3.831321	0.056
3	24.2	696.3	11.605	3.868333	3.870211	0.049
4	33.8	979.0	16.31667	4.079167	4.076782	0.059
5	42.4	1232.0	20.53333	4.106667	4.106500	0.044

Table 3 shows that the discrepancy in determining the rate of jamming a ball in two ways does not exceed 0.06 %. Therefore, the regression analysis method is extremely accurate and makes it possible to investigate the stuck ball (Sommerfeld effect) without visually observing the rotor and the ball.

5. 2. Investigating the Sommerfeld effect with a ball rigidly fixed in the auto-balancer

Fig. 4 shows plots of the acceleration and rotor speed on the run-out of the rotor. The plots are based on a digitized signal (algorithm 3). Recording time is 10 s with a frequency of 5000 measurements per second.

Fig. 4 shows that the rotor has two resonant frequencies. The first is approximately equal to 5 Hz, and the second is 14 Hz.

In total, 100 Excel files were recorded and processed corresponding to 100 different current frequency values and 100 different steady state modes of motion of the system.

Fig. 5 depicts the amplitude-frequency and amplitude-phase characteristics of the rotor, as well as the slip plot of the motor rotor.

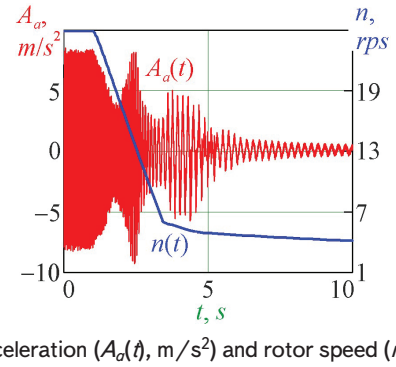

Fig. 4. Acceleration ($A_a(t)$, m/s^2) and rotor speed ($n(t)$, rev/s) plots on the rotor run-out

By peaks in Fig. 5, *a*, two resonant frequencies were found

$$n_{r1} = 5.2381594 \text{ Hz}, \quad n_{r2} = 14.3646154 \text{ Hz}. \qquad (7)$$

The first resonant frequency is responsible for centering the center of mass of the rotor, and the second – for centering at the angle of rotation of the longitudinal axis of the rotor. The second resonance is less pronounced than the first because the ball creates a predominantly static imbalance.

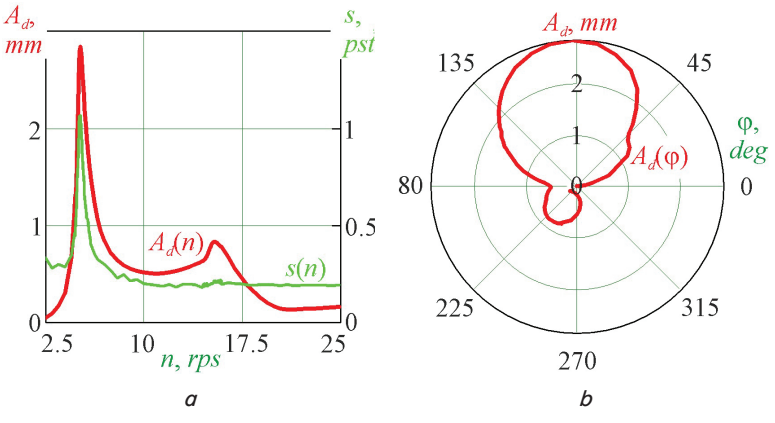

Fig. 5. Determining resonant rotor speeds: *a* – amplitude-frequency characteristic ($A_d(n)$, mm) and rotor sliping (s(*n*), %); *b* – amplitude-phase characteristic ($A_d(\varphi)$, mm)

Fig. 6 shows the dependences on the frequency of the current speed of rotation and sliping of the rotor of the induction motor, and the amplitude of oscillations.

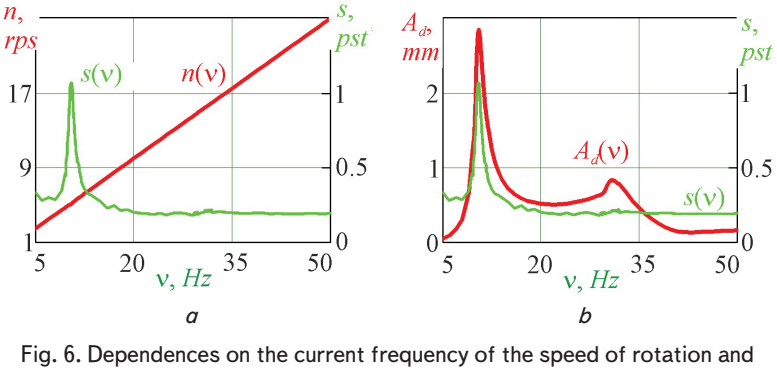

Fig. 6. Dependences on the current frequency of the speed of rotation and sliping of the rotor of the induction motor, and the amplitude of oscillations: *a* – dependence of the rotor speed (*n*, rev/s or Hz) and the sliping of the motor rotor (*s*, %) on the current frequency (ν, Hz); *b* – dependence of the amplitude of oscillations (A_d, mm), and the sliping of the motor rotor (*s*, %) on the current frequency (ν, Hz)

Fig. 6 demonstrates that the sliping of the rotor does not exceed 1.2 %. The peak of sliping comes at the first resonance. On the second resonance, there is no rapid increase in sliping. Consequently, the rotor rotates at a frequency slightly less than half the current frequency. By changing the current frequency (theoretically), it is possible to ensure the rotor rotation at any speed. The Sommerfeld effect is almost not manifested. The peaks of resonances in Fig. 5, *a*, 6, *b* are clearly expressed.

5. 3. Investigating the Sommerfeld effect with a ball freely installed in the auto-balancer

A total of 174 Excel files were recorded and processed, corresponding to 117 different current frequency values and 174 different steady state modes of system motion.

The results of the experiments are shown in Fig. 7. The plots are built on areas where the behavior of the system fundamentally changes.

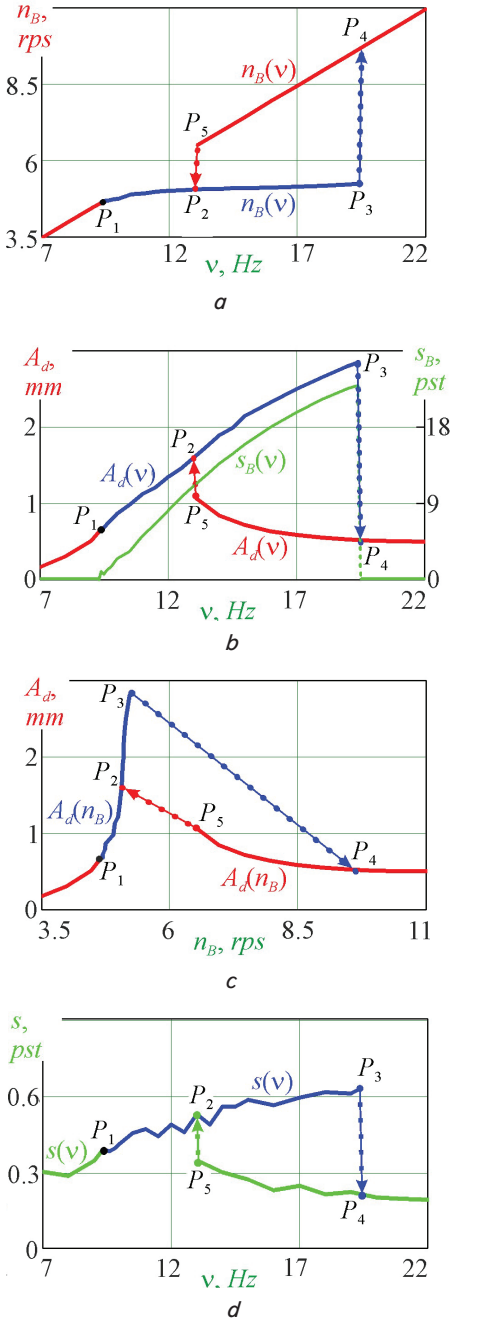

Fig. 7. Results of investigating the Sommerfeld effect with a ball freely installed in the auto-balancer, illustrating qualitative changes in the behavior of the system: *a* – the dependence of the speed of rotation of the ball (n_B, rev/s or Hz) on the current frequency (ν, Hz); *b* – the dependence of the amplitude of oscillations (A_d, mm), and the sliping of the ball (s_B, %) on the frequency of the current (ν, Hz); *c* – the dependence of the amplitude of oscillations (A_d, mm) on the rotational speed of the ball (n_B, rev/s or Hz); *d* – the dependence of the rotor speed (*n*, rev/s or Hz) and the sliping of the motor rotor (*s*, %) on the current frequency (ν, Hz)

Fig. 7, *a* shows the dependence of the speed of rotation of the ball n_B on the current frequency ν. Experiments demonstrate that there are characteristic points and frequency ranges of current.

In the first section, the ball rotates synchronously with the rotor. The section begins with the lowest current frequency (5 Hz) and ends at point P_1, which corresponds to a frequency of 9.3 Hz. The first section coincides with the corresponding part of the plot in Fig. 6, *a*. Therefore, as in Fig. 6, *a*, the line of the section is shown in red.

In the second section, the lag of the ball from the rotor begins and constantly increases. This is a new section and is therefore depicted in blue. The section begins at point P_1 (9.4 Hz) and ends at point P_3 (19.3 Hz).

In the third section, the ball again synchronously rotates with the rotor. In this case, the jump increases the speed of rotation of the ball. There is a transition from point P_3 (19.3 Hz) to point P_4 (19.4 Hz).

The ball rotates synchronously with the rotor at:

– an increase in the current frequency from 19.4 Hz to 50 Hz;

– a reduction of the current frequency from 19.4 Hz (point P_4) to 13.4 Hz (point P_5).

With a decrease in the current frequency from 13.4 Hz to 13.3 Hz, the rotational speed of the ball jump decreases from 6.58 Hz to 5.1 Hz. On the plot, there is a transition from point P_5 to point P_2 in the second section.

Fig. 7, *a* demonstrates that by changing the frequency of the current it is impossible to force the ball to rotate at an arbitrary speed. At point P_3, the ball has a jam speed of 5.24 Hz, which almost coincides with the first resonant frequency. At point P_5, the ball rotates together with the rotor with a frequency of 6.58 Hz. The ball cannot be forced to rotate at speeds lying in the range (5.24, 6.58) Hz.

Fig. 7, *b* shows the dependences of the amplitude of oscillations (A_d, mm), and the sliping of the ball (s_B, %) on the frequency of the current (ν, *Hz*). Comparison with Fig. 6, *b* shows that the rotor has lost a narrow resonant peak between points P_1 and P_5. Instead, a gentle resonant rise P_1–P_2–P_3 appeared. It lasts from 9.4 *Hz* to 19.3 *Hz*. The amplitude on the resonant rise increases from 0.7 mm (point P_1) to 2.84 mm (point P_3).

Fig. 7, *b* demonstrates that the sliping of the ball increases significantly on the resonant rise. It gets stuck at the first resonant speed of rotation of the rotor. The faster the rotor rotates, the closer the ball's rotation frequency is to the resonant frequency, and the greater the amplitude of the rotor's oscillations.

In Fig. 7, *c*, we built amplitude-frequency characteristic for the speed of rotation of the ball. The plot is typical in the case when the rotor rotates a low-power motor [2, 3].

Fig. 7, *d* shows the dependence of the sliping of the motor rotor (*s*, %) on the frequency of the current (ν, *Hz*). Comparison with Fig. 6, *b* reveals that the peak between points P_1 and P_5 disappeared at the sliping of the rotor. Instead, a gentle rise P_1–P_2–P_3 appeared. At point P_3, the rotor slip reaches a maximum of 0.63 %. However, this is almost 2 times less than at the lost peak (1.23 %). Consequently, with the free placement of the ball in the oil, the sliping of the rotor decreased by almost 2 times.

It should be noted that the ball does not get stuck at the second resonant speed, which corresponds to the results reported in [9]. This can be explained by the fact that the ball mainly creates static imbalance, and the momentary component is much smaller.

6. Discussion of results of investigating the phenomenon of ball jam in the ball auto-balancer

The proposed method for studying the Sommerfeld effect in auto-balancers or exciters of resonant vibrations of the pendulum, ball, or roller type demonstrates accuracy and efficiency. To examine the Sommerfeld effect, visual observation of the motion of loads is not required. It is enough to record signals from sensors and process them according to the proposed algorithms using regression analysis methods.

Checking the accuracy of the method using stroboscopic lighting demonstrates the error in determining the rotor speed, ball, rotor oscillation frequency of several hundredths of a percent. The accuracy and reliability of the results of the experiment are increased by conducting all experiments without stopping the bench one after another; processing of recorded signals according to a single algorithm.

When fixing the ball relative to the rotor, a classic inertial vibration exciter is obtained. In the rotor on isotropic viscoelastic resistances, two resonant velocities were found, which corresponds to the general theory of rotary systems. The engine turned out to be powerful enough because the Sommerfeld effect almost did not manifest itself. A gradual increase in the frequency of the current monotonously increases the rotor speed (Fig. 6, *a*). There is no significant slip or jump in the speed of rotor rotation. The amplitude-frequency characteristic (Fig. 5, *a*) has two distinct peaks. Therefore, such a vibration exciter is not suitable by itself for the excitation of resonant vibrations.

With the free placement of the ball in the oil, the behavior of the system changes significantly in the vicinity of the first resonant velocity. The first narrow resonant peak disappears in the rotor (Fig. 6, *b*). Instead, a gentle resonant rise P_1–P_2–P_3 (Fig. 7, *b*) appears. It lasts from 9.4 Hz to 19.3 Hz. The amplitude at the control point on the resonant rise increases from 0.7 mm (point P_1) to 2.84 mm (point P_3). Therefore, by changing the frequency of the current, it is possible to smoothly change the amplitude of the rotor oscillations by almost 4 times. At point P_3, the amplitude of the rotor oscillations is the same as in the first resonance in Fig. 6, *b*.

The ball in the oil in the body of the auto-balancer behaves like an engine whose power is smoothly replaced by a change in the rotor speed of the induction motor (Fig. 7, *c*). Because of this, such a vibration exciter is easy to control. Due to the length of the resonant rise, such a vibration exciter is not very sensitive to changes in the mass of the rotor. It is able to independently excite intense near-resonance vibrations without an external automatic control system.

It should be noted that the studies used one ball of mass of 112 g and one oil grade of medium viscosity. However, the results obtained allow for a certain generalization. The developed research method made it possible to determine with sufficient accuracy the features of the manifestation of the Sommerfeld effect in the ball auto-balancer or the exciter of resonant vibrations. The method is also suitable in the case of resonant vibratory machines with resonant vibration exciters of the pendulum, ball, or roller type. It should be noted that with anisotropy of supports, the rate of sticking of loads fluctuates around a certain average value. This may affect the accuracy of determining the parameters of vibrations by the proposed methods. Therefore, in the future it is planned to investigate with a full-scale experiment the work of a resonant vibration exciter of the pendulum (ball or roller)

type in a single-mass vibratory machine with translational rectilinear motion of the platform.

7. Conclusions

1. The proposed experimental method for studying the Sommerfeld effect in auto-balancers or exciters of resonant vibrations of the pendulum, ball, or roller type demonstrates efficiency and accuracy. To investigate the Sommerfeld effect, it is not necessary to visually observe the motion of loads. It is enough to record signals from sensors and process them according to the proposed algorithms using regression analysis methods. The error in determining the speed of rotor or ball rotation, oscillation frequency of the rotor, etc. does not exceed several hundredths of a percent.

The accuracy and reliability of the results of the experiment are increased by conducting all experiments without stopping the bench one after another; processing of recorded signals according to a single algorithm.

2. When fixing the ball relative to the rotor, a classic inertial vibration exciter is obtained. In the rotor on isotropic viscoelastic resistances, two resonant velocities were found, which corresponds to the general theory of rotary systems. The engine turned out to be powerful enough as the Sommerfeld effect almost did not manifest itself. A gradual increase in the frequency of the current monotonously increases the rotor speed. There is no significant slip or jump in the rotor speed. There are two distinct peaks on the amplitude-frequency characteristic. Therefore, such a vibration exciter is not suitable for the excitation of resonant vibrations in itself.

3. With the free placement of the ball in the oil, the behavior of the system changes significantly in the vicinity of the first resonant velocity. The rotor loses the first narrow resonant peak. Instead, there is a long, gentle resonant rise. It lasts from 9.4 Hz to 19.3 Hz. The amplitude at the reference point on the resonant rise increases from 0.7 mm to 2.84 mm. Therefore, by changing the frequency of the current, it is possible to smoothly change the amplitude of the rotor oscillations by almost 4 times. The maximum amplitude of oscillations of the rotor is the same as at the first resonance with a fixed ball.

The ball in the oil in the body of the auto-balancer behaves like an engine, the power of which is smoothly replaced by a change in the speed of rotation of the induction motor. Because of this, such a vibration exciter is easy to control. Due to the flatness of the resonant rise, such a vibration exciter is not very sensitive to changes in the mass of the rotor. It is able to independently excite intense near-resonance vibrations without an external automatic control system.

Conflict of interest

The authors declare that they have no conflict of interest in relation to this research, whether financial, personal, authorship or otherwise, that could affect the research and its results presented in this paper.

Acknowledgements

This paper is funded within scientific work No. 0122U002077 “Theoretical foundations for the creation of resonant vibration exciters and resonant vibratory machines of wide purpose, working on the Sommerfeld effect and the phenomenon of self-synchronization”, carried out at the Central Ukrainian National Technical University using the general fund of the state budget.

References

1. Sommerfeld, A. (1902). Beiträge zum dynamischen Ausbau der Festigkeitslehre. Zeitschrift des Vereines Deutscher Ingenieure, 46, 391–394.
2. Blekhman, I. I. (2000). Vibrational mechanics: nonlinear dynamic effects, general approach, applications. World Scientific, 536. doi: https://doi.org/10.1142/4116
3. Kononenko, V. O., IGladwell, G. M. L. (Ed.) (1969). Vibrating systems with a limited power supply. London: Iliffe, 236.
4. Balthazar, J. M. (Ed.) (2022). Nonlinear Vibrations Excited by Limited Power Sources. Springer Nature, 422. doi: https://doi.org/10.1007/978-3-030-96603-4
5. Yaroshevich, N., Puts, V., Yaroshevich, T., Herasymchuk, O. (2020). Slow oscillations in systems with inertial vibration exciters. Vibroengineering PROCEDIA, 32, 20–25. doi: https://doi.org/10.21595/vp.2020.21509
6. Samantaray, A. (2021). Efficiency considerations for Sommerfeld effect attenuation. Proceedings of the Institution of Mechanical Engineers, Part C: Journal of Mechanical Engineering Science, 235 (21), 5247–5260. doi: https://doi.org/10.1177/0954406221991584
7. Lanets, O. V., Shpak, Ya. V., Lozynskyi, V. I., Leonovych, P. Yu. (2013). Realizatsiia efektu Zommerfelda u vibratsiinomu maidanchyku z inertsiinym pryvodom. Avtomatyzatsiia vyrobnychykh protsesiv u mashynobuduvanni ta pryladobuduvanni, 47, 12–28. Available at: http://nbuv.gov.ua/UJRN/Avtomatyzac_2013_47_4
8. Kuzo, I. V., Lanetc, O. V., Gurskii, V. M. (2013). Synthesis of low-frequency resonance vibratory machines with an aeroinertia drive. Naukovyi visnyk Natsionalnoho hirnychoho universytetu, 2, 60–67. Available at: http://nbuv.gov.ua/UJRN/Nvngu_2013_2_11
9. Ryzhik, B., Sperling, L., Duckstein, H. (2004). Non-synchronous Motions Near Critical Speeds in a Single-plane Autobalancing Device. Technische Mechanik, 24, 25–36. Available at: https://journals.ub.uni-magdeburg.de/index.php/techmech/article/view/911
10. Lu, C.-J., Tien, M.-H. (2012). Pure-rotary periodic motions of a planar two-ball auto-balancer system. Mechanical Systems and Signal Processing, 32, 251–268. doi: https://doi.org/10.1016/j.ymssp.2012.06.001

11. Jung, D. (2018). Supercritical Coexistence Behavior of Coupled Oscillating Planar Eccentric Rotor/Autobalancer System. Shock and Vibration, 2018, 1–19. doi: https://doi.org/10.1155/2018/4083897
12. Drozdetskaya, O., Fidlin, A. (2021). Passing through resonance of the unbalanced rotor with self-balancing device. Nonlinear Dynamics, 106 (3), 1647–1657. doi: https://doi.org/10.1007/s11071-021-06973-4
13. Artyunin, A. I., Eliseyev, S. V. (2013). Effect of "Crawling" and Peculiarities of Motion of a Rotor with Pendular Self-Balancers. Applied Mechanics and Materials, 373-375, 38–42. doi: https://doi.org/10.4028/www.scientific.net/amm.373-375.38
14. Artyunin, A. I., Barsukov, S. V., Sumenkov, O. Y.; Radionov, A., Kravchenko, O., Guzeev, V., Rozhdestvenskiy, Y. (Eds.) (2020). Peculiarities of Motion of Pendulum on Mechanical System Engine Rotating Shaft. Proceedings of the 5th International Conference on Industrial Engineering (ICIE 2019). ICIE 2019. Lecture Notes in Mechanical Engineering. Cham: Springer, 649–657. doi: https://doi.org/10.1007/978-3-030-22041-9_70
15. Filimonikhin, G., Yatsun, V. (2015). Method of excitation of dual frequency vibrations by passive autobalancers. Eastern-European Journal of Enterprise Technologies, 4 (7 (76)), 9–14. doi: https://doi.org/10.15587/1729-4061.2015.47116
16. Filimonikhin, G., Yatsun, V., Filimonikhina, I., Ienina, I., Munshtukov, I. (2019). Studying the load jam modes within the framework of a flat model of the rotor with an autobalancer. Eastern-European Journal of Enterprise Technologies, 5 (7 (101)), 51–61. doi: https://doi.org/10.15587/1729-4061.2019.177418
17. Yatsun, V., Filimonikhin, G., Podoprygora, N., Pirogov, V. (2019). Studying the excitation of resonance oscillations in a rotor on isotropic supports by a pendulum, a ball, a roller. Eastern-European Journal of Enterprise Technologies, 6 (7 (102)), 32–43. doi: https://doi.org/10.15587/1729-4061.2019.182995
18. Varanis, M., Balthazar, J. M., Silva, A., Mereles, A. G., Pederiva, R. (2018). Remarks on the Sommerfeld effect characterization in the wavelet domain. Journal of Vibration and Control, 25 (1), 98–108. doi: https://doi.org/10.1177/1077546318771804
19. Yatsun, V., Filimonikhin, G., Nevdakha, A., Pirogov, V. (2018). Experimental study into rotational-oscillatory vibrations of a vibration machine platform excited by the ball auto-balancer. Eastern-European Journal of Enterprise Technologies, 4 (7 (94)), 34–42. doi: https://doi.org/10.15587/1729-4061.2018.140006